Original article

A Study on Determination of an Optimized Detector for Single Photon Emission Computed Tomography

Mohammad Khoshakhlagh, Jalil Pirayesh Islamian[1], Mohammad Abedi[2], Babak Mahmoudian[3], Ali Reza Mardanshahi[2]

Immunology Research Center, Tabriz University of Medical Sciences, [1]Departments of Medical Physics, Faculty of Medicine and [3]Department of Radiology, Radiotherapy and Nuclear Medicine, Faculty of Medicine, Tabriz University of Medical Sciences, Tabriz, [2]Department of Radiology, Faculty of Medicine, Mazandaran University of Medical Sciences, Sari, Iran

Abstract

The detector is a critical component of the single photon emission computed tomography (SPECT) imaging system for giving accurate information from the exact pattern of radionuclide distribution in the target organ. The SIMIND Monte Carlo program was utilized for the simulation of a Siemen's dual head variable angle SPECT imaging system with a low energy high resolution (LEHR) collimator. The Planar and SPECT scans for a ^{99m}Tc point source and a Jaszczak Phantom with the both experiment and simulated systems were prepared and after verification and validation of the simulated system, the similar scans of the phantoms were compared (from the point of view of the images' quality), namely, the simulated system with the detectors including bismuth germanate (BGO), yttrium aluminum garnet (YAG:Ce), Cerium-doped yttrium aluminum garnet (YAG:Ce), yttrium aluminum perovslite (YAP:Ce), lutetium aluminum garnet (LuAG:Ce), cerium activated lanthanum bromide (LaBr3), cadmium zinc telluride (CZT), and sodium iodide activated with thallium [NaI(Tl)]. The parameters of full width at half maximum (FWHM), energy and special resolution, sensitivity, and also the comparison of images' quality by the structural similarity (SSIM) algorithm with the Zhou Wang and Rouse/Hemami methods were analyzed. FWHMs for the crystals were calculated at 13.895, 14.321, 14.310, 14.322, 14.184, and 14.312 keV and the related energy resolutions obtained 9.854, 10.229, 10.221, 10.230, 10.131, and 10.223 %, respectively. Finally, SSIM indexes for comparison of the phantom images were calculated at 0.22172, 0.16326, 0.18135, 0.17301, 0.18412, and 0.20433 as compared to NaI(Tl). The results showed that BGO and LuAG: Ce crystals have high sensitivity and resolution, and better image quality as compared to other scintillation crystals.

Keywords: Gamma detector, Jaszczak Phantom, SIMIND simulation, structural similarity algorithm

Introduction

Single photon emission computed tomography (SPECT) imaging studies the distribution of an administered radiotracer *in vivo*. The images are strongly affected by the attenuation, scattering, and response of the detector. The conventional detector is mainly made from sodium iodide activated by thallium [NaI(Tl)] in nuclear medicine imaging. In SPECT, the used radioisotopes mainly decay by gamma irradiation, with the energy ranging from 50 KeV to 511 KeV. On the other hand, the favorite detector should have some characteristics such as high energy resolution, appropriate photon conversion efficiency, high density, short decay time, short radiation length as well as appropriate physical strength, with least afterglow, in order to obtain images with the best quality for a proper diagnosis.[1] Bismuth germanate (BGO), due to its better sensitivity and higher density[2] with a low afterglow and also as a nonhygroscopic crystal was suggested as a proper candidate for radioisotopic imaging.[3] BGO crystal is commonly used in positron emission tomography (PET) scanners for its high photo fraction that is needed in PET imaging.[4] However, yttrium aluminum garnet (YAG: Ce) and Cerium-doped yttrium aluminum perovskite (YAP: Ce) have the benefit of an average density but YAP: Ce also has

Access this article online

Quick Response Code:

Website: www.wjnm.org

DOI: 10.4103/1450-1147.167588

Address for correspondence:
Dr. Jalil Pirayesh Islamian, Department of Medical Physics, Faculty of Medicine, Tabriz University of Medical Sciences, Tabriz, Iran. E-mail: pirayeshj@gmail.com

energy resolution better than YAG: Ce.[5] On the other hand, YAG: Ce has the ability to detect x-rays and low energy gamma ray photons. Also, cerium-doped lutetium aluminum garnet (LuAG: Ce) has higher density than YAG: Ce and faster decay time than BGO crystal.[6] Cerium activated lanthanum bromide (LaBr3) has a good energy resolution and low decay time with a high temperature stability also at room temperature.[5-7] A new crystal, cadmium zinc telluride (CZT) with a high density, very short decay time, and excellent energy resolution were recently suggested in the optical and nuclear medicine imaging systems. CZT crystal significantly reduces imaging time owing to its very short decay time, and it also administered the dosage of the patients in nuclear medicine imaging.[8] This study planned to compare the abovementioned crystals for an optimized SPECT imaging [Table 1].

Materials and Methods

Monte Carlo simulation

The SIMIND Monte Carlo program was used for simulating Siemen's dual head variable angle SPECT imaging system with seven detectors, including BGO, YAG:Ce, YAP:Ce, LuAG:Ce, LaBr3, CZT, and NaI(Tl), a ^{99m}Tc point source, and also a Jaszczak Phantom. The program is freely downloadable from the site: www.radfys.lu.se/simind. The SIMIND program mainly consists of two programs: CHANGE that defines the system and scanning parameters and SIMIND that performs the actual simulation. The program can also simulate a nonuniform attenuation from voxel-based phantoms and includes several types of variance reduction techniques.[9]

Phantom studies

A ^{99m}Tc point source and an acrylic cylindrical Jaszczak Deluxe Phantom[10] were used for both the experiment and the simulation studies. The ^{99m}Tc point source has been considered to have an activity of 37 MBq, with an isotropic source emitting 140 keV gamma photons. Moreover, the acrylic cylindrical Jaszczak Deluxe Phantom, with the spherical inserts measuring 9.5 mm, 12.7 mm, 15.9 mm, 19.1 mm, 25.4 mm, and 31.0 mm in diameter and the inserts of rods measuring 4.8 mm, 6.4 mm, 7.9 mm, 9.5 mm, 11.1 mm, and 12.7 mm diameter were filled with a uniform solution of 370 MBq ^{99m}Tc. As the SIMIND simulated SPECT projections are noise-free, for realization the noise was added according to the administered dose.[11] The phantom is used for routine quality assurance and control, including system spatial resolution, contrast, and uniformity.[9] The experiment and also the simulated SPECT of the phantom were generated. The acquisition parameters were matrix of 128 × 128, 128 views, 1.23 zoom factor, and 3.9 mm pixel size, and the images were reconstructed with the filtered back projection reconstruction using a Butterworth filter with an order of 5 and in cutoff frequency of 0.25. The qualities of the produced images were compared in terms of image contrast and spatial resolution.[9-12]

Quantitative image evaluation

The structural similarity (SSIM) algorithm has two methods for a quantitative image evaluation, namely Zhou Wang and Rouse/Hemami. The SSIM metric calculates various windows of an image. The measure between two images x and y of common size N × N is:

$$SSIM(x;y) = \frac{(2\mu_x\mu_y + C_1)(2\sigma_{xy} + C_2)}{(\mu_x^2 + \mu_y^2 + C_1)(\sigma_x^2 + \sigma_y^2 + C_2)}$$

Where μ_x is the average of x and μ_y is the average of y, σ_x^2 is the variance of x and σ_y^2 is the variance of y. σ_{xy} is the covariance of x and y. $C_1 = (k_1L)^2$ and $C_2 = (k_2L)^2$ are two variables to stabilize the division with a weak denominator. L is the dynamic range of the pixel values (L = 255 for 8 bits/pixel gray scale images) and finally, $k_1 = 0.01$ and $K_2 = 0.03$ by default.[13,14]

Results

Point source simulation

Figure 1 shows the energy spectra produced by the experiment and simulated gamma cameras from a ^{99m}Tc point source. Some minor differences may be observed between the simulated and the experimental energy spectra; the experimental spectrum presents a wider peak that may be explained by the superimposition of the energy peaks with the x-ray energy of ^{99m}Tc.[15] Also, Figure 2 shows energy spectra for the related ^{99m}Tc point source scans by the simulated system with the detectors of BGO, YAG: Ce, YAP: Ce, LuAG: Ce, LaBr3, and CZT crystals. Contributions of the Compton and photoelectric interactions in the whole spectra (simulated) and in the selected window, and also some functional parameters are given in Table 2.

Table 1: Certain quantities of the crystals may be used as nuclear medicine detectors

	NaI(Tl)	BGO	YAG:Ce	YAP:Ce	LuAG:Ce	CZT	LaBr3
Density (g/cm^3)	3.67	7.13	4.55	5.37	6.76	5.78	5.08
Light output (%NaI(Tl))	100	15-20	40	60	20	-	160
Decay time (ns)	230	300	70	25	70	1	26
Energy resolution (% at 661 keV)	7.2	12	7.2	6.7	6.7	0.5	2.7

BGO: Bismuth germanate; NaI (Tl): Sodium iodide activated with thallium; YAG:Ce: Yttrium aluminum garnet; YAP:Ce: Yttrium aluminum perovslite; LuAG:Ce: Cerium-doped lutetium aluminum garnet; CZT: Cadmium zinc telluride

Table 2: Results of some functional parameters for the simulation of a ^{99m}Tc point source scanning with BGO, YAG:Ce, YAP:Ce, CZT, LuAG:Ce, and LaBr3 crystals

Parameter detector	FWHM (mm)	FWHM (keV)	Energy resolution (%)	Sensitivity (cps/MBq)	Peak to compton	Scatter to primary ratio	Scatter to total ratio	Efficiency (peak)	Efficiency (detector)
NaI (Tl)	7.287	13.906	9.9327	79.7930	4.6888	0.5910E-02	0.5876E-02	0.7398	0.9260
BGO	7.182	13.895	9.8545	91.8050	7.4274	0.5825E-02	0.5791E-02	0.8524	1.0000
YAG: Ce	7.728	14.321	10.229	48.2099	1.6654	0.6237E-02	0.6198E-02	0.4483	0.7348
YAP: Ce	7.665	14.310	10.221	58.6133	2.2813	0.6084E-02	0.6047E-02	0.5443	0.8044
LuAG: Ce	7.226	14.322	10.230	86.7538	4.9858	0.5794E-02	0.5760E-02	0.8050	0.9988
LaBr3	7.476	14.184	10.131	81.9677	5.0699	0.5970E-02	0.5935E-02	0.7596	0.9392
CZT	7.203	14.312	10.223	90.3213	6.6055	0.5824E-02	0.5790E-02	0.8385	0.9993

The Jaszczak SPECT Phantom provides consistent performance information for any SPECT or PET system. BGO: Bismuth germanate; NaI(Tl): Sodium iodide activated with thallium; YAG:Ce: Yttrium aluminum garnet; YAP:Ce: Yttrium aluminum perovslite; LuAG:Ce: Cerium-doped lutetium aluminum garnet; CZT: Cadmium zinc telluride

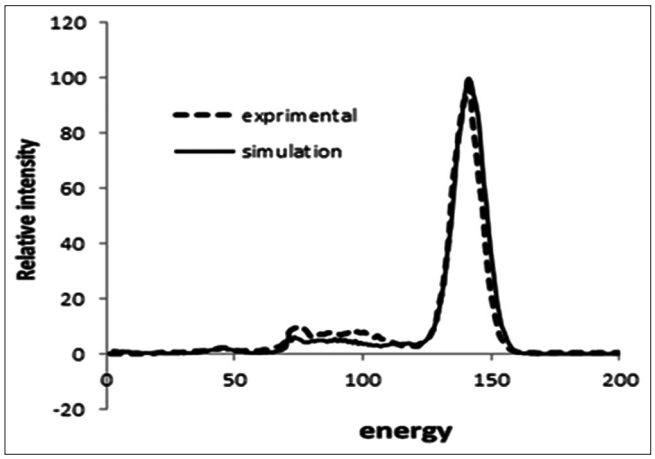

Figure 1: Energy Spectra of the simulated (solid) and experiment (dashed) ^{99m}Tc point source scanning with NaI(Tl) detector

Jaszczak Phantom simulation

In this study, we simulated SPECT scanning of the hot and cold Jaszczak Phantoms and compared the related experiment and simulated reconstruction images with the SSIM algorithm by the Zhou Wang and Rouse/Hemami methods. The methods gave suitable information on comparing the images from the point of view of image contrast, luminance, and structure as well as provided a multiscale-SSIM (MS-SSIM) similarity index [Table 3]. The same comparisons were done for the images after changing the crystals of the simulated SPECT system with CZT, LaBr3, LuAG: Ce, YAG: Ce, YAP: Ce, and BGO [Table 4]. The quality of the resultant images in Figures 3 and 4 have shown the acquisition of pie slice of the simulated hot and cold Deluxe Phantoms by SPECT with the seven detectors.

Table 3: The data on comparing cold Jaszczak Phantom pie slice images with SSIM algorithm, and the Zhou Wang and Rouse/Hemami methods for the experimented and simulated reconstructed SPECT images of the phantom

Method image parameter	Zhou Wang	Rouse/Hemami
Luminance comparison	0.98254	0.99001
Contrast comparison	0.98458	0.98271
Structure comparison	0.98113	0.98681
MS-SSIM	0.98279	0.98793

MS-SSIM: Multiscale-structural similarity

Discussion

SIMIND as a Monte Carlo program has benefits in the simulation of the hardware of SPECT. The effects of scintillator crystal on the performance parameters, sensitivity, and efficiency as well as the results of quantitative and qualitative analysis of reconstructed SPECT images have been studied in the present research. We simulated the SPECT system with NaI (Tl) and six different crystals, including CZT, LaBr3, LuAG: Ce, YAG: Ce, YAP: Ce, and BGO. Figure 1 shows the energy spectra of the simulated and experiment ^{99m}Tc point sources scanned with NaI(Tl) detector. Angela *et al*. (2011) studied the LaBr3 crystal *in vivo* for the administration of radioiodine (I-131) in the thyroid gland to obtain acceptable results and consequently enunciated it as an appropriate detector. The properties that make the LaBr3:Ce scintillator detector attractive for different applications based on γ-ray spectrometry include very suitable energy resolution and very fast light decay, enabling high count rate applications, high temperature stability, high gamma detection efficiency, stability at room temperature, and promising technology for manufacturing the crystal at larger sizes.[7] Furthermore, Liu B *et al*. reviewed the BGO crystal that has occupied more than 50% of the PET market.[1] In this regard, Derenzo *et al*. compared the NaI (Tl) crystal with the BGO crystal and found the latter to be more sensitive mainly due to its higher density.[16] Our results [Table 2] also showed that BGO crystals have higher sensitivity, 91.8050 cps/MBq with full width at half maximum (FWHM) of 13.895 KeV, and peak/Compton 7.4274 with a lower energy resolution 9.8545 (%) than other crystals. In addition, Lo Meo Sergio *et al*. studied some nuclear medicine crystals and have determined that LuAG: Ce with energy resolution of 6.7 and 70 ns decay time is better than BGO.[17] Also, Chewpraditkul W *et al*. demonstrated that LuAG: Ce has better detection rate than YAG:Ce from

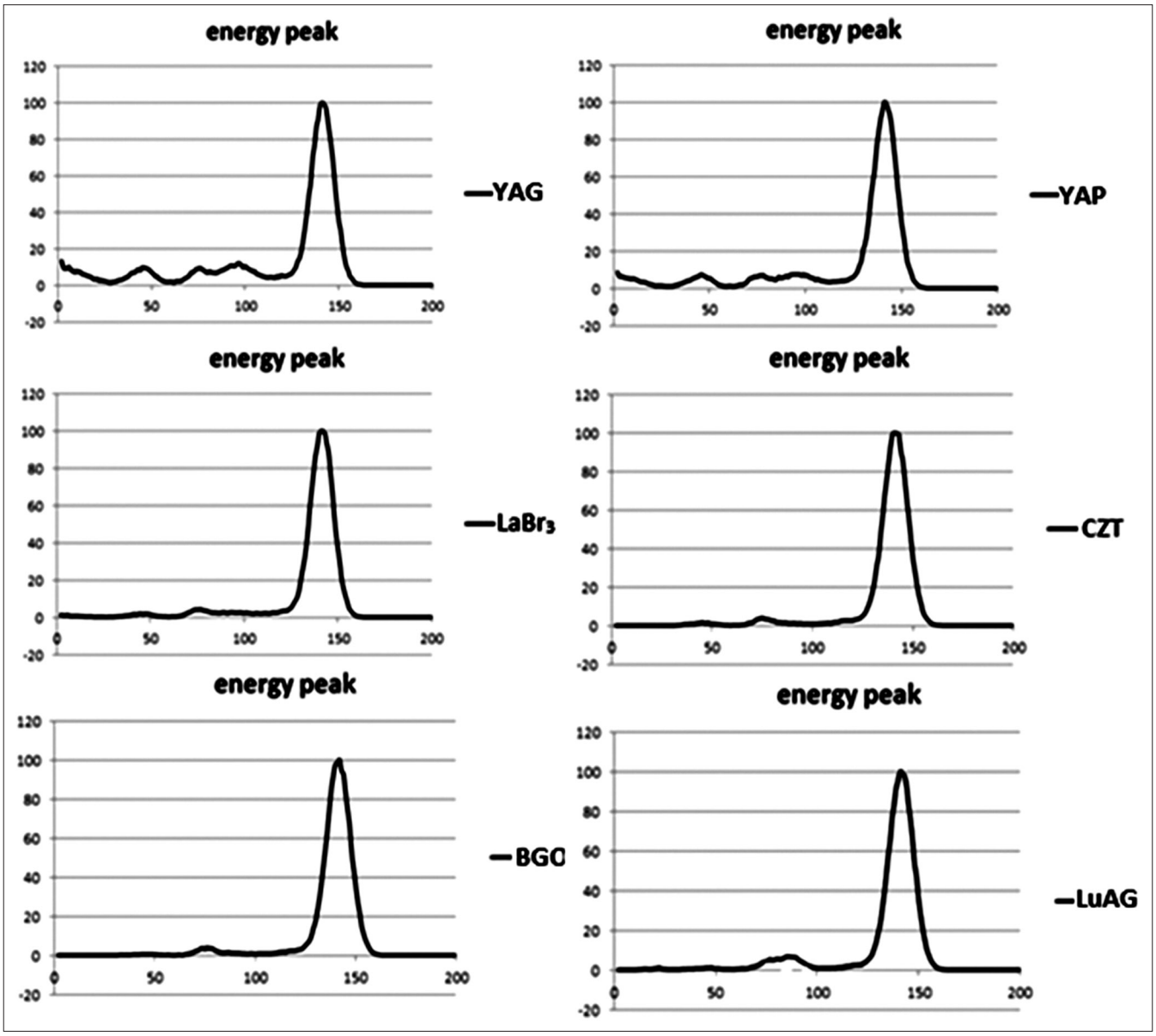

Figure 2: Energy spectra from simulation of a ^{99m}Tc point source scanning with BGO, YAG:Ce, YAP:Ce, CZT, LuAG:Ce, and LaBr3 crystals

Table 4: The data on comparison of pie slice images from a hot Jaszczak Phantom scanning with BGO, YAG: Ce, YAP: Ce, CZT, LuAG: Ce, and LaBr3 crystals by SSIM algorithm and the Zhou Wang and Rouse/Hemami methods

Crystal parameter	BGO	YAG:Ce	YAP:Ce	LuAG:Ce	LaBr3	CZT
Luminance comparison	0.99345	0.98125	0.99287	0.99723	0.99321	0.99299
Contrast comparison	0.98982	0.98735	0.98927	0.98983	0.98912	0.98972
Structure comparison	0.22548	0.16851	0.18463	0.17527	0.18742	0.20791
MS-SSIM index Zhou Wang	0.22172	0.16326	0.18135	0.17301	0.18412	0.20433
Luminance comparison	0.99341	0.98112	0.99282	0.99718	0.99312	0.99292
Contrast comparison	0.98909	0.98667	0.98854	0.98931	0.98842	0.98903
Structure comparison	0.21472	0.15557	0.17249	0.16440	0.17576	0.19677
MS-SSIM index Rouse/Hemami	0.21097	0.15060	0.16929	0.16219	0.17253	0.19323

BGO: Bismuth germanate; YAG:Ce: Yttrium aluminum garnet; YAP:Ce: Yttrium aluminum perovslite; LuAG:Ce: Cerium-doped lutetium aluminum garnet; CZT: Cadmium zinc telluride; MS-SSIM: Multiscale-structural similarity

the point of view of higher density (6.76 g/cm^3) and higher atomic number (58.9).[6] In our study, we used SSIM algorithm for comparing the simulated with the experimental Jaszczak Phantom reconstructed images.

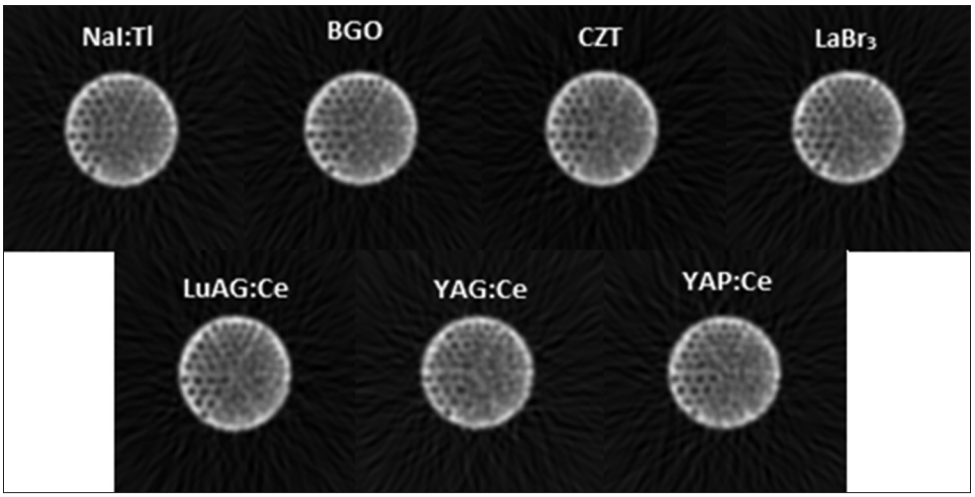

Figure 3: Images from the simulated SPECT of cold Jaszczak Phantom acquisition, consisting of 148 rods with 10 mCi ^{99m}Tc by BGO, YAG:Ce, YAP:Ce, CZT, LuAG:Ce, and LaBr3 crystals

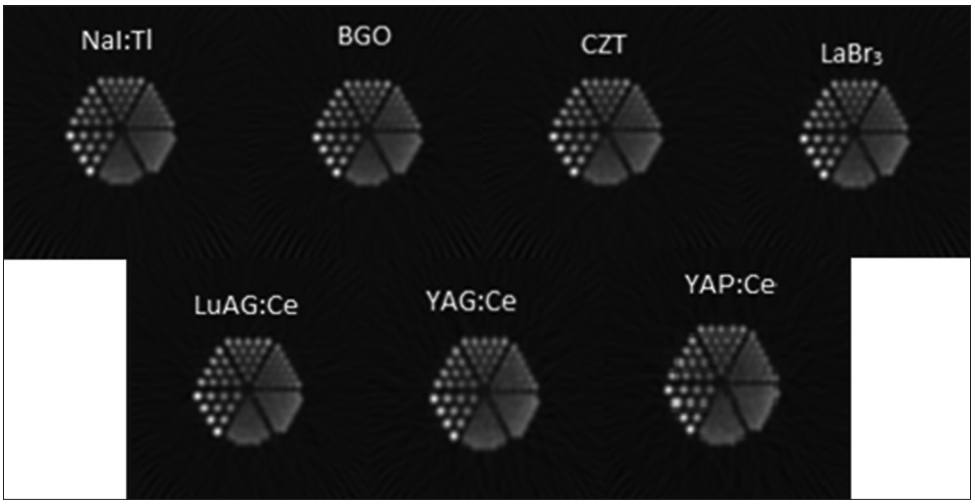

Figure 4: Images from the simulated SPECT of hot Jaszczak Phantoavm acquisition, consisting of 148 rods with 10 mCi ^{99m}Tc by BGO, YAG:Ce, YAP:Ce, CZT, LuAG:Ce, and LaBr3 crystals

Table 3 shows the MS-SSIM numbers of 0.98279 and 0.98793 for the hot Jaszczak Phantom images with the Zhou Wang and Rouse/Hemami methods, respectively. Meanwhile, we changed the crystal material during the simulation of Jaszczak Phantom and studied images' quality in six scintillator crystals, including BGO, YAG: Ce, YAP: Ce, LuAG: Ce, LaBr3, and CZT. The related SSIM algorithms were obtained with MS-SSIM numbers 0.22172, 0.16326, 0.18135, 0.17301, 0.18412, and 0.20433 by the Zhou Wang method and 0.21097, 0.15060, 0.16929, 0.16219, 0.17253, and 0.19323 by the Rouse/Hemami method for a quantity study of the simulation images of the Jaszczak Phantom. However, these results show the LuAG: Ce detector with some more different MS-SSIM numbers and also with some difference in quality between the Jaszczak Phantom images and the other crystals.

Conclusion

The poor resolution of SPECT has impaired its use in clinical practice.[14] It is well known that the best detector with a high fast process can provide beneficial effect for better diagnosis and reduce the time of scans. The results of our current study showed that the BGO crystal is more sensitive than other crystals [Table 2]. Moreover, the Zhou Wang and the Rouse/Hemami methods for hot Jaszczak Phantom images showed that LuaG: Ce and CZT crystals have good images for the smallest visible rods of the hot Jaszczak Phantom [Figure 4] and also that LuAG: Ce crystals provide better images, determined with SSIM algorithms [Table 4]. These data might encourage the planning of studies in more detail and allow users to have a better investigation compared to other equipments commonly utilized in nuclear medicine.

Acknowledgment

The authors are grateful to the head and all staff members of the Nuclear Medicine department of Fathemeh Zahra Hospital of Sari University of Medical Sciences for their sincere cooperation. This work was financially supported by the Immunology Research Center of Tabriz University of Medical Sciences, Tabriz, Iran.

References

1. Liu B, Shi C. Development of medical scintillator. Chin Sci Bull 2002;47:1057-63.
2. BGO Bismuth germinates scintillation material. Available from: http://www.crystals.Saint-gobain.coms. [Last accessed on 2014 Apr 03].
3. Holly TA, Abbott BG, Al-Mallah M, Calnon DA, Cohen MC, DiFilippo FP, *et al*; American Society of Nuclear Cardiology. Single photon-emission computed tomography. J Nucl Cardiol 2010;17:941-73.
4. Madsen MT. Recent advances in SPECT imaging. J Nucl Med 2007;48:661-73.
5. Moszynski M, Kapusta M, Zalipska J, Balcerzyk M, Wolski D, Szawlowski M, *et al*. Low energy γ-rays scintillation detection with large area avalanche photodiodes. IEEE Trans Nucl Sci 1999;46:880-5.
6. Chewpraditkul W, Swiderski L, Moszynski M, Szczesniak T, Syntfeld-Kazuch A, Wanarak C, *et al*. Scintillation properties of LuAG:Ce, YAG:Ce and LYSO:Ce crystals for gamma-ray detection. IEEE Trans Nucl Sci 2009;56(6):3800-5.
7. Saizu MA, Cata-Danll G. Lanthanum bromide scintillation detector for gamma spectrometry applied in internal radioactive contamination measurements. UPB Sci Bull 2011;73:119-26.
8. CZT Technology: Fundamentals and Applications. Available from: http://www3.gehealthcare.com. [Last accessed on 2014 Dec 09].
9. Islamian JP, Bahreyni Toossi MT, Momennezhad M, Naseri S, Ljungberg M. Simulation of a quality control Jaszczak phantom with SIMIND Monte Carlo and adding the phantom as an accessory to the program. Iran J Med Phys 2012;9:135-40.
10. Groch MW, Erwin WD. Single-photon emission computed tomography in the year 2001: Instrumentation and quality control. J Nucl Med Technol 2001;29:12-8.
11. Islamian JP, Toossi MTB, Momennezhad M, Zakavi SR, Sadeghi R. Monte Carlo Study of the Effect of Backscatter Material Thickness on 99mTc Source Response in Single Photon Emission Computed Tomography. Iran J Med Phys 2013;10:1-2:69-77.
12. Holstensson M, Hindrof C, Ljungberg M, Partridge M, Flux GD. Optimization of energy-window setting for scatter correction in quantitative (111) In imaging: Comparison of measurements and Monte Carlo simulations. Cancer Biother Radiopharm 2007;22:136-42.
13. Wang Z, Bovik AC, Sheikh HR, Simoncelli EP. Image Quality Assessment: From Error Visibility to Structural Similarity. IEEE Trans Image Process 2004;13:600-12.
14. Islamian JP, Toossi MT, Momennezhad M, Zakavi SR, Sadeghi R, Ljungberg M. Monte carlo study of the effect of collimator thickness on T-99m source response in single photon emission computed tomography. World J Nucl Med 2012;11:70-4.
15. Bahreyni Toossi MT, Islamian JP, Momennezhad M, Ljungberg M, Naseri SH. SIMIND Monte Carlo simulation of a single photon emission CT. J Med Phys 2010;35:42-7.
16. Derenzo SE, Budinger TF, Huesman RH, Cahoon JL, Vuletich T. Imaging properties of a positron tomograph with 280 Bgo crystals. IEEE Trans Nucl Sci 1981;28:81-9.
17. Lo Meo S, Baldazzi G, Bennati P, Bollini D, Cencelli VO, Cinti MN, *et al*. Optical physics of scintillation imagers by GEANT4 simulations. Nucl Instr Meth Phys Res A 2009;607:259-60.

How to cite this article: Khoshakhlagh M, Islamian JP, Abedi M, Mahmoudian B, Mardanshahi AR. A study on determination of an optimized detector for single photon emission computed tomography. World J Nucl Med 2016;15:12-7.

Source of Support: This study was financially supported by the Immunology Reserch Center of Tabriz University of Medical Sciences. The authors owe special thanks to Professor Michael Ljungberg for providing the detectors input files for SIMIND simulation, and also to the Department of Nuclear Medicine in Fatemeh Zahra Hospital of Sari, Iran. **Conflict of Interest:** None declared.